

Document downloaded from:

<http://hdl.handle.net/10251/162243>

This paper must be cited as:

Tampau, A.; González Martínez, MC.; Chiralt Boix, MA. (2020). Biodegradability and disintegration of multilayer starch films with electrospun PCL fibres encapsulating carvacrol. *Polymer Degradation and Stability*. 173:1-8.
<https://doi.org/10.1016/j.polymdegradstab.2020.109100>



The final publication is available at

<https://doi.org/10.1016/j.polymdegradstab.2020.109100>

Copyright Elsevier

Additional Information

Biodegradability and disintegration of multilayer starch films with electrospun PCL fibres encapsulating carvacrol

Alina Tampau ^{1a}, Chelo González-Martínez ^{2b}, Amparo Chiralt ^{3c}

^{a, b, c} Instituto Universitario de Ingeniería de Alimentos para el Desarrollo, Ciudad Politécnica de la Innovación, Universitat Politècnica de Valencia, Camino de Vera, s/n, 46022 Valencia, Spain.

¹ altam@upv.es, ² cgonza@tal.upv.es, ³ dchiralt@tal.upv.es

1 Abstract

2 The biodegradation and disintegration of thermoplastic starch multilayers containing carvacrol(CA)-
3 loaded poly-(ϵ -caprolactone) electrospun mats were evaluated under thermophilic composting
4 conditions for 45 and 84 days, respectively, and compared with non-loaded carvacrol films and pure
5 starch films. Sample mass loss, thermogravimetric and visual analyses were performed throughout
6 the disintegration test. The disintegration behaviour of all multilayers was similar, reaching values
7 of 75-80 % after 84 days. Biodegradation, assessed by carbon dioxide measurements, revealed
8 that all the carvacrol-free films completely biodegraded after 25 composting days. However, the
9 presence of CA notably affected the compost inoculum activity, thus limiting the biodegradability of
10 the CA-loaded multilayers to a maximum value of around 85 % after 45 days. Nevertheless, this
11 value was close to that established by the standard ISO method to qualify as biodegradable
12 material.

13 **Keywords:** thermoplastic starch; poly-(ϵ -caprolactone); carvacrol; TGA; disintegration;
14 biodegradation.

15

16 **Abbreviations:** EFSA, European Food Safety Authority; S, starch; PCL, poly-(ϵ -caprolactone); CA,
17 carvacrol; GAA, glacial acetic acid; MCC, microcrystalline cellulose; TGA, thermogravimetric
18 analysis; DTGA, derivative thermogravimetric analysis; SSR, synthetic solid residue; DS, dry solids;
19 VS, volatile solids; MC, moisture content;

20 1. Introduction

21 The quantity of plastics produced in the first 10 years of the current century is likely to approach the
22 quantity produced in the entire preceding century [1] and only a modest percentage of these

¹ Corresponding autor details:

Mailing address: Instituto Universitario de Ingeniería de Alimentos para el Desarrollo, Ciudad Politécnica de la Innovación, building 8E Access F, L0-03, Universitat Politècnica de Valencia, Camino de Vera, s/n, 46022 Valencia, Spain.

E-mail address: altam@upv.es

23 packaging materials ends up being recycled (plastic recycling rates of 9.1% in the US in 2015 [2]
24 and 40.9% in the EU in 2016 [3]). The usage and disposal of plastics is controversial and there are
25 growing concerns about waste accumulation, problems for wildlife resulting from ingestion and the
26 potential for plastics to transfer harmful chemicals to wildlife and humans. There are numerous
27 studies alerting to the alarming levels of microplastics found in oysters [4], mussels [5],[6],[7] crabs
28 [8] and fish [9], [10] which move up through the food chain, ending up in the human body. Risk
29 assessments developed by the European Food Safety Authority (EFSA) [11] have taken these
30 considerations into account. However, perhaps the most important overriding concern is that our
31 current usage is not sustainable [1].

32 Due to the environmental impact these plastics generate owing to their long degradation times,
33 more effort is being made to develop packaging from biodegradable materials. This trend is aligned
34 with consumer demand for more natural products for food contact materials. As a result, new
35 materials have been developed, using biodegradable polymers from renewable sources, such as
36 polysaccharides and proteins, and natural active agents of plant or marine origin.

37 Starch (S) is one of the most commonly studied, readily available carbohydrates, obtainable from
38 renewable sources at relatively low cost. Starch films present very good oxygen barrier capacity,
39 but due to their hydrophilic nature, films exhibit water sensitivity and poor water vapour barrier
40 properties. Combining, in multilayer assemblies, starch layers with sheets of hydrophobic polymers
41 - with high water vapour barrier capacity - would provide these materials, intended for food
42 packaging, with more adequate barrier capacity for both water vapour and oxygen. In this sense,
43 poly-(ϵ -caprolactone) (PCL) (a completely biodegradable aliphatic polyester) [12] has been
44 combined with thermoplastic corn starch, forming bilayers with improved barrier properties when
45 compared to neat starch films [13], [14]. These multilayer films became active films with
46 antimicrobial properties by incorporating carvacrol encapsulated into electrospun PCL layers [14].
47 The encapsulation of carvacrol in PCL mats by electrospinning showed better retention of the
48 compound in this non-polar matrix, exhibiting higher encapsulation efficiency than starch [15].
49 Likewise, electrospinning is applied at room temperature which also contributes to preserve the
50 compound against the potential deterioration and volatilization that can occur during the starch
51 thermal processing. Carvacrol (CA) is a phenolic monoterpene, one of the major constituents of
52 oregano and thyme essential oils [16]. It exhibits significant *in vitro* antimicrobial [17], [18], [19] and
53 antioxidant activity [20], [21], and has been approved as a food additive by Joint FAO/WHO [22]
54 and as flavouring substance by EFSA [23]. It is currently being used as a bioactive in packaging
55 materials [24], [25], [26]. Thus, the addition of active compounds to biopolymer layers confers
56 antimicrobial and/or antioxidant properties, making these materials more attractive as food
57 packaging candidates. Given the inhibiting effect of such antimicrobial compounds on microflora, it
58 is likely that the biodegradation of these matrices could be altered by the presence of active
59 compounds [27], [28].

60 Composting is a form of organic recycling, based on the activity of the microbiota population, which
61 breaks down the biodegradable parts of the waste, generating stabilized organic residue [29]. The
62 resulting compost could be used as soil conditioner to increase soil productivity by replenishing
63 some of its nutrients, and reduce the excessive use of synthetic fertilizers [27]. As pointed out by
64 Balaguer et al. [27], not all biodegradable polymers are compostable, since compostability implies
65 biodegradation by biological processes at a rate consistent with other known compostable
66 materials, leaving non-visibly distinguishable or toxic residues. Therefore, evaluation of
67 compostability includes three phases: disintegration, biodegradation and ecotoxicity. The
68 biodegradability and compostability of developed active packaging materials made with
69 biodegradable polymers can be affected by the presence of actives or blend interactions and cannot
70 be assumed as such. It must be analysed to ensure that the newly created materials comply with
71 the requirements specified by law [29].

72 The aim of this study is to assess the disintegration and biodegradation behaviour under laboratory
73 composting conditions of starch-PCL multilayer films, incorporating or not carvacrol.

74

75 **2. Materials and experimental design**

76 **2.1. Materials**

77 Starch for film preparation was provided by Roquette Laisa España S.A. (Benifaió, Valencia, Spain),
78 while PCL pellets (average M_n 80,000), CA and glacial acetic acid (GAA) were obtained from Sigma-
79 Aldrich (Sigma–Aldrich Chemie, Steinheim, Germany).

80 For the biodegradation and disintegration studies, ripe compost (no older than 4 months) was
81 offered by a local solid residue treatment plant (Valencia, Spain). Other components used for the
82 disintegration test consisted of urea (Urea 46% Prill, Tarazona, Spain), sawdust (Productos de
83 Limpieza Adrian, Almacera, Valencia, Spain), corn starch (Roquette Laisa España S.A. (Benifaió,
84 Valencia, Spain), rabbit-feed (Super Feed S.L., Madrid, Spain), saccharose (White sugar,
85 Azucarera Ebro, Madrid, Spain) and corn seed oil (Hacendado brand, Mercadona supermarkets,
86 Spain). For the biodegradation test, vermiculite from a local market was used. Microcrystalline
87 cellulose (MCC) (powder, 20 μm) was purchased from Sigma Aldrich Química S.L., Madrid, Spain.
88 Magnesium nitrate ($\text{Mg}(\text{NO}_3)_2$) and Phosphorous pentoxide (P_2O_5) used for creating controlled
89 relative humidity environments for sample storage were purchased from Panreac Química S.A.
90 (Castellar de Valles, Barcelona, Spain).

91

92 **2.2. Films preparation**

93 The starch films were prepared by compression moulding, following the protocol described
94 previously by Tampau et al. [14]. Briefly, a mixture of starch : glycerol : water=1 : 0.3 : 0.5 (wt. / wt.)
95 was processed in a two-roll mill (Model LRM-M-100, Labtech Engineering, Thailand) at 160 °C and
96 8 rpm for 30 minutes. The resulting pellets were conditioned for one week at 25 °C in a desiccator

97 with saturated $\text{Mg}(\text{NO}_3)_2$ aqueous solution, to ensure a 53 % relative humidity. Each individual
98 starch film was obtained from 4 grams of conditioned pellet, moulded by thermo-compression in a
99 press (Model LP20, Labtech Engineering, Thailand), at 50 bars / 160 °C for 2 min, then at 130 bars
100 / 160 °C for 6 min and cooled down to 50 °C for 3 min.

101 Multilayer films were prepared by coating one side of a starch film with an electrospun layer
102 (application time of 90 minutes, voltage 15.0 kV, flow-rate 1.2 mL/h , distance needle-collector 15
103 cm) of a PCL solution (15 % wt. / wt.) in GAA with or without CA (15 g carvacrol / 100 g PCL),
104 following the methodology described by Tampau et al. [14], using a Fluidnatek Biolnacia (Valencia,
105 Spain) equipment. Later on, the PCL-coated starch films were thermo-compressed with another
106 neat starch film at 130 bars / 80 °C for 4 min followed by a cooling at 50 °C for 2 min. Thus, three
107 multilayer films were obtained: starch-starch (SS), starch-PCL-starch (SPS) and starch-PCL-starch
108 containing carvacrol in the PCL layer (SPCAS). Thermocompression under the described
109 conditions gave rise to a good layer adhesion in normal conditions, although these layers partially
110 detached when starch sheets swelled under high moisture conditions, in which these films would
111 not be applicable.

112

113 **2.3. Samples characterization**

114 **2.3.1. Moisture content, elemental composition and visual appearance**

115 Prior to the tests, the multilayer films were analysed as to their moisture content (as described by
116 Cano et al. [28]) and thickness, measured in 5 different points using a Palmer digital micrometre
117 (Comecta, Barcelona, Spain). In order to determine the C, N and H composition of the samples, an
118 elemental analysis was performed by means of a Euro EA3000 analyser (EUROVECTOR, Milan,
119 Italy). Analyses were carried out in triplicate.

120 The visual changes that samples presented throughout the disintegration experiments were
121 analysed. For this purpose, specific samples extracted from the reactors at different times were
122 previously dried in a vacuum oven at 40 °C for a week. Pictures were taken by means of a digital
123 camera (EOS 5D Mark II, Canon, Japan).

124 **2.3.2. Thermogravimetric analysis**

125 The samples were submitted to a thermogravimetric analysis (TGA) at different times of the
126 composting process (day 0, 14, 21, 42 and 84). Prior to this analysis, the composted samples were
127 conditioned by drying in a vacuum oven at 40 °C for one week and later transferred to a desiccator
128 with P_2O_5 until constant weight. A TGA/SDTA 851e analyser (Mettler Toledo, Schwarzenbach,
129 Switzerland) working under nitrogen flow (20 mL / min) was used to obtain the weight loss curves
130 vs. temperature (TGA) and the first derivatives (DTGA). Between 5 and 10 mg of conditioned
131 sample was placed in a 70 μL alumina crucible and heated from 25 to 600 °C at 10 K / min. With
132 the software provided by the Mettler Toledo analyser, the onset, peak and end temperatures of the
133 degradation steps were obtained. All measurements were done in triplicate.

134 **2.4. Compost and synthetic solid residue (SSR)**

135 The ripe compost (acting as the inoculum) was prepared by removing any inert pieces like shards
136 of glass and stones, and then sieved. Its pH was assessed by mixing 1 part compost to 5 parts
137 deionized water and measured immediately, to ensure a value between 7 and 9.

138 Following the ISO 20200 International Standard (2004) [30], a synthetic solid residue (SSR) was
139 prepared for the disintegration test, by manually mixing the required components described in
140 section 2.1. For the purpose of the biodegradation test, the inoculum was just mixed with vermiculite
141 to prevent compacting and thus ensuring good oxygenation. For both tests, the water content was
142 adjusted to 55 % (wt. / wt.) by adding de-ionized water and gently stirring. This ensured the compost
143 was moist, but without visible free water.

144 The SSR was characterized as to its dry solids (DS) and volatile solids (VS) content, as specified
145 by ISO 20200 [30], both at the beginning, as well as at the end of the composting process (84 days).
146 The DS was determined by drying the analysed sample in an oven at 105 °C until constant mass
147 was reached and expressed as a percentage of the total mass of the analysed sample. The VS was
148 obtained from the previously dried sample by calcination at 550 °C in a muffle (Selecta, Barcelona,
149 Spain) until constant weight, and expressed as a percentage with respect to the DS. The ripe
150 compost used for the biodegradation study was also characterized in terms of DS and VS at initial
151 time.

152 **2.5. Disintegration test**

153 Disintegration test was carried out in the laboratory, following the International Standard guidelines
154 [30]. Roughly 10 grams of film samples (cut into 25 x 25 mm squares) were placed with 1 kg of wet
155 SSR in each composting unit (reactor) consisting of a polypropylene box with lid. On each one of
156 the narrow sides of the reactor, one hole (5 mm in diameter) was made at approximately 6.5 cm
157 from the bottom, to allow gas exchange between the inside and outside atmospheres. The filled
158 reactors were placed in an oven (Selecta, J.P. Selecta S.A., Barcelona, Spain) at 58 ± 2 °C to ensure
159 controlled thermophilic conditions. Their initial weight was recorded and was closely monitored
160 throughout the duration of the essay (84 days), restoring it totally or partially with de-ionised water,
161 as specified by the aforementioned ISO standard [30]. Three reactors per formulation were
162 prepared, each reactor containing less than 10 g total mass of samples included in mesh bags (1 x
163 1 mm mesh size). One of these samples with around 5 g (cut into 25 x 25 mm squares) was used
164 to control the sample weight loss at the final time, according to the standard guidelines, and the
165 other mesh bags, each with only one sample square (25 x 25 mm, about 0.3 g) were extracted from
166 the reactor at different control times in order to carry out the TGA and visual analysis (described in
167 section 2.3), and the weight control. Prior to these analyses, the mesh bags containing samples
168 were gently cleaned with a soft brush to eliminate the adhered compost residues. The disintegration
169 percentage after 84 days ($D_{84}(\%)$) was calculated by means of the **eq. 1**:

170

$$D_{84}(\%) = \frac{m_0 - m_{84}}{m_0} \cdot 100 \quad \text{[eq. 1]}$$

171 where m_0 is sample dry mass at the start of test and m_{84} is dry mass of the final disintegrated
172 samples after 84 composting days.

173

174 2.6. Biodegradation test

175 The starch films containing electrospun PCL material were also submitted to an aerobic
176 biodegradation assessment under controlled composting conditions following the guidelines of the
177 ISO 14855-1 standard method [31], as adapted by other authors [27] and [28] by mixing the non-
178 activated vermiculite and compost to prevent the compost compaction and ensure good oxygen
179 access. The principle of this method assumes that the CO_2 that forms during the biodegradation of
180 a sample is directly proportional to the carbon percentage that is biodegraded from that respective
181 sample. The test was performed inside airtight glass jars of 2000 mL in volume, whose lids were
182 modified with a covered septum. Inside the jars, 2 polypropylene cups were placed: one containing
183 3 g of dry compost mixed with 1 g of vermiculite and a sample quantity (previously cut in 2 mm²
184 squares) equivalent to 50 mg of carbon, while the second one, contained water to ensure 100%
185 relative humidity inside the jar. The samples were maintained up to 45 days at 58±2 °C. A control
186 sample was also prepared using MCC as reference material [27]. A blank sample contained just
187 compost with vermiculite. The percentage of CO_2 generated inside the reactors was measured in
188 triplicate using a CO_2 analyser (CheckMate 9900 PBI Dansensor, Ringsted, Denmark) throughout
189 the biodegradation process.

190 The theoretical amount of CO_2 that could be generated from the sample ($\text{CO}_2^{\text{Th}}_S$) was estimated
191 from its carbon content applying **eq. 2**. The biodegradation percentage (B%) at each time was
192 calculated as the ratio between the cumulative amounts of CO_2 produced by the sample throughout
193 the 45 days with respect to the theoretical amount ($\text{CO}_2^{\text{Th}}_S$), applying **eq. 3** [31].

194

$$\text{CO}_2^{\text{Th}}_S = DW_S \cdot C_S \cdot \frac{Mw_{\text{CO}_2}}{Mw_C} \quad \text{[eq. 2]}$$

195

$$B\% = \frac{\sum \text{CO}_{2S} - \sum \text{CO}_{2B}}{\text{CO}_2^{\text{Th}}_S} \quad \text{[eq. 3]}$$

196 where:

197 - DW_S is the dry weight of sample (g);

198 - C_S is the percentage of carbon in the dry sample, as determined by elemental analysis (%);

199 - Mw_{CO_2} and Mw_C are the molecular weights of CO_2 and of C respectively;

200 - $\sum \text{CO}_{2S}$ is the cumulative amount of carbon dioxide in the sample reactors at each time throughout
201 test period (g);

202 - $\sum \text{CO}_{2B}$ is the cumulative amount of carbon dioxide detected in the blank reactor at each time (g).

203 The experimental data obtained from the biodegradation test was modelled using Hill's equation
204 **(eq.4)** in order to describe the kinetics of the process.

205
$$B\% = B\%_{max} \cdot \frac{t^n}{k^n + t^n}$$
 [eq. 4]

206

207 Where:

208 - $B\%_{max}$ is the percentage of biodegradation at infinite time (%);

209 - t is the time (days);

210 - k is the time at which $0.5B\%_{max}$ has occurred;

211 - n is the curve radius of the sigmoid function.

212 2.7. Statistical analysis

213 All statistical analysis were performed through analysis of variance (ANOVA) using the application
 214 STATGRAPHICS Centurion XVI (Statgraphics Technologies, Inc., The Plains, Virginia 20198,
 215 USA). Fisher's least significant difference (LSD) procedure was used at the 95% confidence level.

216

217 3. Results

218 3.1. Properties of multilayer films

219 **Table 1** presents the properties of the starch film samples prior to the tests. As can be observed,
 220 while the films presented similar moisture content values among formulations, the presence of the
 221 electrospun layer of PCL significantly increased the film thickness and the carbon content of these
 222 multilayers, according to the presence of PCL with higher C ratio in the molecule. The thickness of
 223 multilayer films notably increased with respect to the usual thickness of monolayer films. [32].

224

225 **Table 1.** Samples' moisture content (MC), thickness and elemental carbon (C %) analysis prior to
 226 the composting test. Mean values and standard deviation.

| Sample / reactor | MC (%) | Thickness (μm) | C % |
|------------------|--------------------------------|-----------------------------|------------------------------|
| SS | 6.73 \pm 0.16 ^{ab} | 430 \pm 30 ^a | 40.4 \pm 0.2 ^a |
| SPS | 6.59 \pm 0.16 ^a | 500 \pm 30 ^b | 41.2 \pm 0.6 ^{ab} |
| SPCAS | 6.956 \pm 0.010 ^b | 490 \pm 20 ^b | 42.3 \pm 1.3 ^b |

227 Different superscript letters (a, b, c...) in the same column indicate significant differences ($p < 0.05$) among samples

228 3.2. Compost characteristics

229 The active compost used as inoculum for both tests presented a pH of 8.25 (measured according
 230 to the ISO method), total dry solids (DS) content of 70 \pm 1 % and organic matter content of 56 \pm 1 %
 231 (expressed as volatile solids (VS) with respect to the dry solids). Characteristics of the pre-
 232 composting SSR prepared for the disintegration test are shown in **Table 2**. The volatile solids
 233 content decreased slightly at the end of the composting process with respect to the initial value, as
 234 an indicator of the organic matter being converted into CO₂ by the compost microflora. Then, the
 235 test was validated taking into account the standard method, which established a reduction of the

236 volatile content in the sample after the composting period (R values, **Table 2**) of over 30 % as well
 237 as the standard deviation of the disintegration values of the samples (D_{84} (%), in **Table 2**) lower than
 238 10 units. Likewise, throughout the duration of the test, the colour changes described by the ISO
 239 20200 standard [30] were observed in the compost (from lighter yellow (due to sawdust presence)
 240 to a darker brown). The odour of the compost was strongly ammoniacal within the first week, and it
 241 disappeared gradually, according to that described in ISO 20200 standard [30].

242

243 **Table 2.** Volatile solids VS (g volatiles / 100 g compost DS) before and after the composting period
 244 of the disintegration test, the difference between these values (R: expressed as % with respect to
 245 the initial value) and disintegration percentage for the samples. Mean values and standard
 246 deviations.

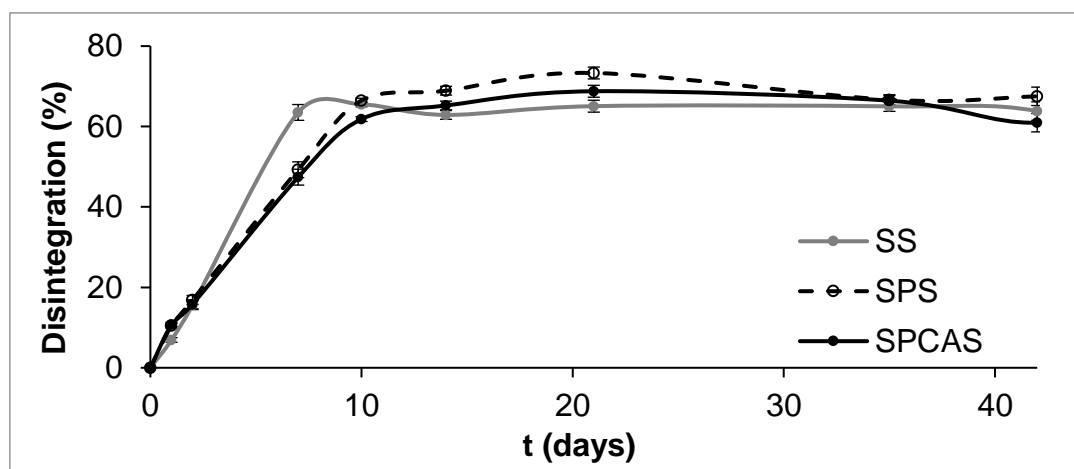
| Reactor | VS (g / 100 g DS) | | R (%) | Disintegration D_{84} (%) |
|-------------|----------------------|-----------------------|--------------------|--------------------------------|
| | Pre composting | Post composting | Decrease in VS | |
| SSR (blank) | 95.0±0.3 | 91.3±0.6 ^c | 43±1 ^a | - |
| SS | | 80.5±0.7 ^a | 55±1 ^b | 75±6 ^a |
| SPS | | 85.9±1.1 ^b | 52± 2 ^b | 81.1±0.5 ^a |
| SPCAS | | 84.5±0.5 ^b | 51± 2 ^b | 75±4 ^a |

247 Different superscript letters (a,b,c...) in the same column indicate significant differences ($p < 0.05$) among samples.

248 3.3. Disintegration test







249 The degree of disintegration (D) of films when exposed to laboratory-scale composting
 250 environmental conditions (58±2 °C for 84 days) provided information about the physical breakdown
 251 of films into smaller fractions. **Figure 1** shows the disintegration values as a function of time for the
 252 different samples. As shown, all films presented similar disintegration patterns taking into account
 253 the uncertainty associated with the sample mass control. It is difficult to ensure the lack of compost
 254 particles in the sample and the complete delivery of the disintegrated sample particles from the
 255 mesh, since under moist environment these remain stuck/agglomerated and compacted under the
 256 mechanical action of the mesh. Similar asymptotic values were attained for the different samples
 257 (75-80 %) after about 14 days, although the final values shown in **Table 2** correspond to the samples
 258 introduced in the reactor for the purpose of this control, according to standard guidelines, at the end
 259 of the test period (84 days). The mass fluctuations throughout the asymptotic period can be
 260 attributed to the different amounts of adhered compost particles or to different losses of
 261 disintegrated sample particles through the mesh. The visual appearance of the samples at different
 262 composting times is also presented in **Figure 2**. It is remarkable that about 14 days only were
 263 required to disintegrate the films as can be deduced from both **Figures 1** and **2**. In fact, the visual
 264 appearance of the samples at 14 days corresponded to agglomerated particles with certain degree

265 of compactness due to the high moisture content in the reactor and the mechanical protection/action
 266 of the mesh.
 267



268
 269 **Figure 1.** Development of sample disintegration as a function of time for the different multilayer
 270 films. (Mean values and LSD intervals ($p < 0.05$)).

271 Non-significant differences ($p < 0.05$) in the D_{84} (%) values were found among samples at the end of
 272 the composting period, being the mean D_{84} (%) value 77 ± 5 %. These values are in agreement with
 273 those mentioned by Castro-Aguirre et al. [33] for trays with similar composition. As reported by
 274 Balaguer et al. [27], the erosion kinetics are affected by two major factors: 1) the water diffusion
 275 through the polymer layer and 2) the rate of degradation of the polymeric chains. Other authors [28]
 276 observed higher disintegration rates for starch films obtained by casting which could be attributed
 277 to differences in the films thickness and polymer arrangements in the film structure obtained by
 278 different processing methods. Nevertheless, this disintegration process in the obtained bilayer films
 279 was very similar according to their similar specific surface. This permits the water diffusion and
 280 uptake, favouring the microbial action and bulk erosion, thus breaking the matrix in small fragments.

| day | Sample | | |
|-----|---|---|--|
| | SS | SPS | SPCAS |
| 0 |  |  |  |
| 1 |  |  |  |



281 **Figure 2.** Visual appearance of the samples throughout the disintegration period.

282 The degradation degree of polymer throughout the disintegration period has been analysed via
 283 thermogravimetric analysis at different times. **Figure 3** shows TGA and DTGA curves obtained for
 284 the films at different times and **Table 3** gives the onset and peak temperatures for the degradation
 285 steps of the samples at initial and final time of the disintegration test. As can be observed in **Figure**
 286 **3**, samples presented a first degradation step at around 61-63 °C (T_p), corresponding to the
 287 evaporation of bound water. This step was not detected in the samples at initial time ($t=0$), which
 288 suggests that the partially degraded samples exhibit greater water binding capacity due to the
 289 changes in the mean molecular weight or composition of the substrate. The main peak
 290 corresponding to the starch degradation showed the maximum degradation rate at T_p around 280-
 291 290 °C, in agreement with the value reported by Collazo-Bigliardi et al. [34] for starch films.
 292 However, it is remarkable that the peak became wider and split throughout the composting period.
 293 This reflects the formation of starch subunits of lower molecular weight that degrade at lower
 294 temperature, as has been observed by other authors [35], [36]. The mass loss profiles (DTGA
 295 curves) slightly vary for the different multilayers. This suggests differences in the degradation
 296 mechanisms in each case, depending on the presence of PCL and carvacrol. The degradation step
 297 of electrospun PCL at about 360 °C (as described by Tampau et al. [14]) only appeared in the initial
 298 samples, and it was no longer observed in samples at 14 days of the process. This suggests most
 299 of the PCL polymer chains were quickly broken down by the composting bacteria due to the low
 300 thickness (less than 60 μm) of the electrospun layer and the possible detachment of the multilayer

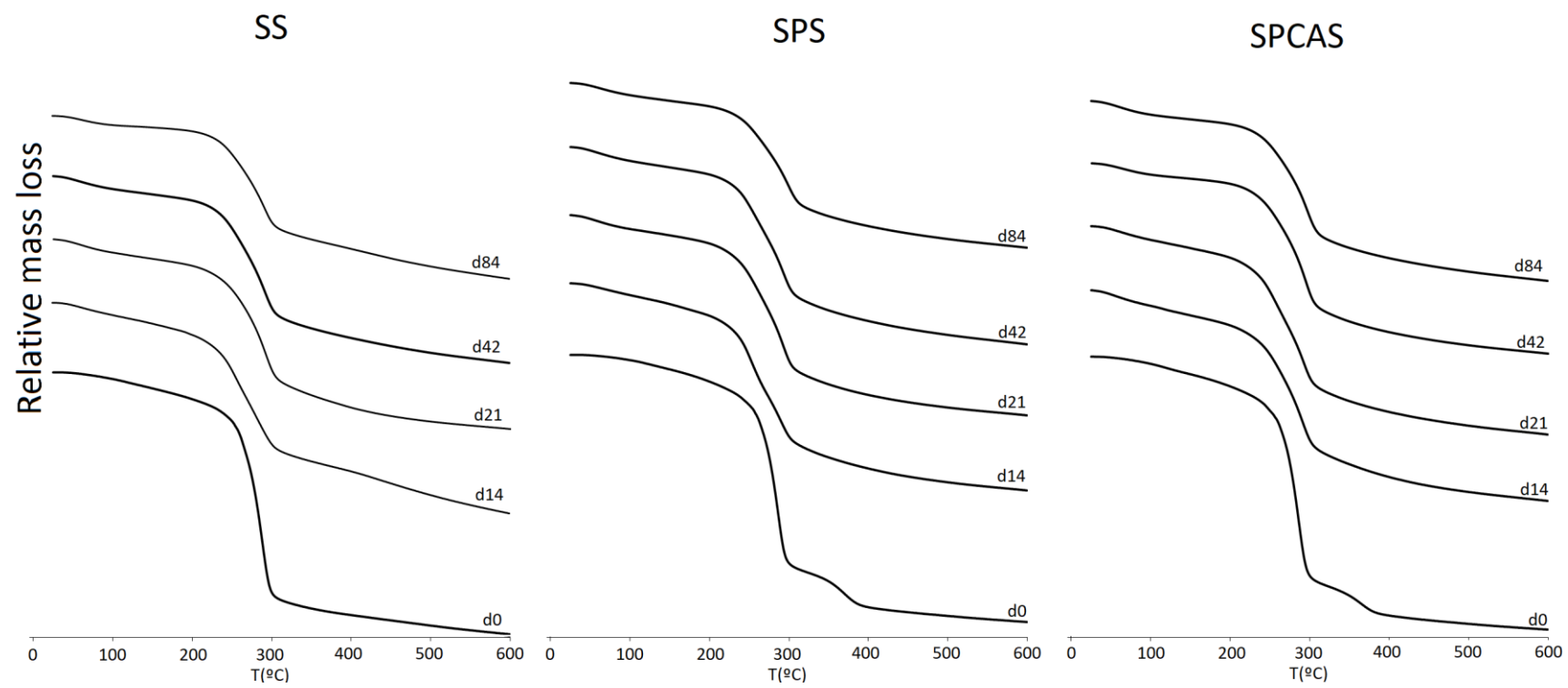
301 assembly, promoted by the starch swelling in the wet compost environment, which increases the
 302 specific surface area of the PCL sheet and the disintegration's effectiveness. There was no thermo-
 303 released carvacrol detected for the samples submitted to TGA analysis at different times of the
 304 disintegration process. This can be due to its low mass fraction in the bilayer (about 0.5), as reported
 305 in a previous study [14].

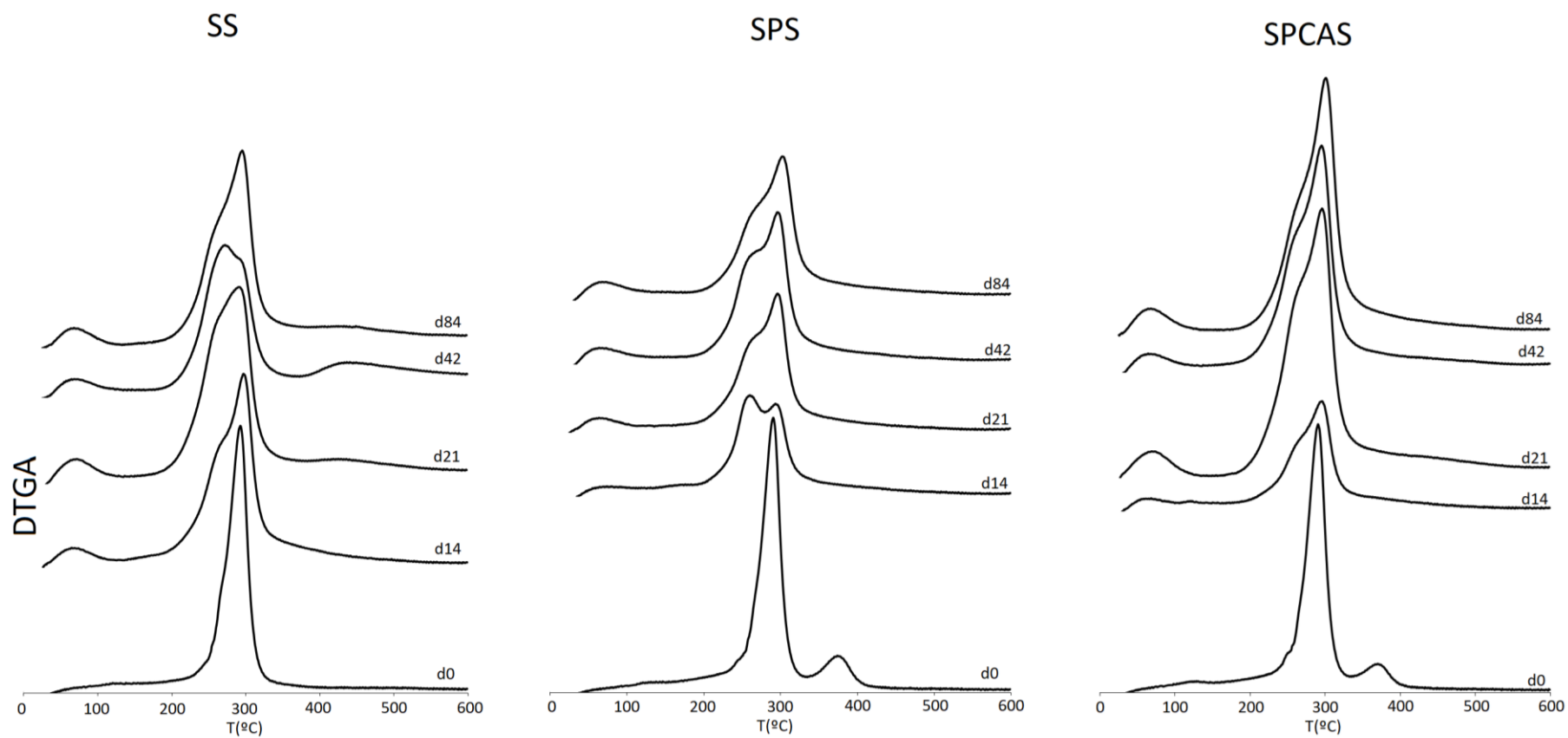
306 The percentage of residual mass at 600 °C is also presented in **Table 3**. All initial samples showed
 307 low values for this parameter, which significantly ($p < 0.05$) increased after the composting period.
 308 The increase in the residual mass after 84 days can be fully justified by disappearance of the organic
 309 fraction of the sample (forming CO₂, N₂, CH₄, and H₂O) during biodegradation, with the subsequent
 310 increase of mass fraction of mineral content, as observed by other authors [28]. However, sample
 311 contamination with compost particles could also contribute to the increase in the residue.

312 **Table 3.** TGA parameters obtained for the pre- and post- composting samples: onset (T_o), peak
 313 (T_p), endset (T_e) temperatures, and pyrolysis residual mass at 600 °C. Different superscript letters
 314 in the same column indicate significant differences ($p < 0.05$) among samples.

| Sample | Day | 1 st step | | | 2 nd step | | 3 rd step | | Residual mass (%) |
|--------|-----|----------------------|-------------------|--------------------|----------------------|--------------------|----------------------|--------------------|-------------------|
| | | T _o | T _p | T _e | T _o | T _p | T _o | T _p | |
| SS | 0 | - | - | - | 257±1 ^b | 286±2 ^b | - | - | 3±3 ^a |
| | 84 | 37±4 ^a | 63±1 ^a | 109±3 ^a | 223±11 ^a | 290±1 ^c | - | - | 34±5 ^b |
| SPS | 0 | - | - | - | 244±2 ^b | 281±1 ^a | 331±15 ^a | 366±5 ^a | 6±1 ^a |
| | 84 | 39±4 ^a | 62±3 ^a | 104±4 ^a | 227±15 ^a | 293±2 ^d | - | - | 37±4 ^b |
| SPCAS | 0 | - | - | - | 244±1 ^b | 282±1 ^a | 321±28 ^a | 362±8 ^a | 5±2 ^a |
| | 84 | 37±4 ^a | 61±4 ^a | 105±3 ^a | 243±6 ^b | 293±1 ^d | - | - | 34±2 ^b |

315



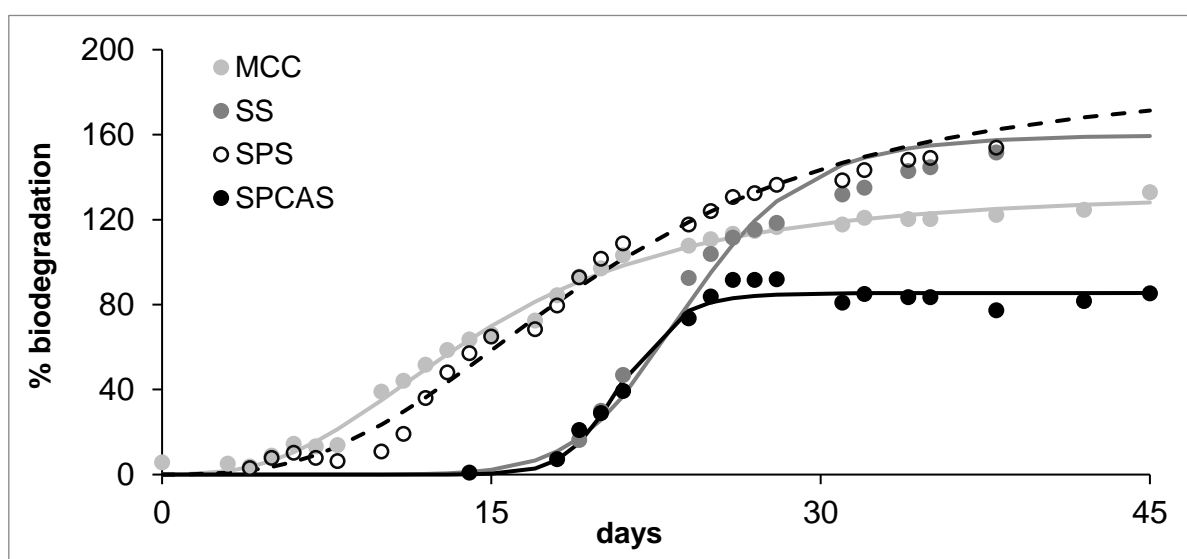


317 **Figure 3.** TGA and DGTA curves of starch multilayer films submitted to the disintegration process at different composting times (0, 14, 21, 42
 318 and 84 days).

319 3.4. Biodegradation test

320 The samples' biodegradability potential was assessed in a laboratory setup by direct measurement
321 of the CO₂ generated during aerobic composting at 58±2 °C for 45 days. The compostable material
322 is used by microorganisms as an energy source for their metabolic activities and cellular growth, which
323 under aerobic conditions means the transformation of the samples' carbon into CO₂. The maximum
324 amount of CO₂ that could be generated from the samples was theoretically calculated based on the
325 carbon content (**Table 1**) previously determined through elemental analysis.

326 **Figure 4** presents the biodegradation kinetics of the starch based multilayers and the microcrystalline
327 cellulose used as reference material. All samples exhibited the typical sigmoid profile of the
328 respirometric test in agreement with other studies [27], [28]. An initial lag period lasting among 4-18
329 days, depending on the sample, was observed. This period length is affected by the
330 adaptation/selection time of microorganisms and the time where the degree of material degradation
331 reached about 10 % of the maximum. The presence of carvacrol in SPCAS sample and the higher
332 adhesion forces of starch sheets in SS sample (that increased the effective sample thickness) seemed
333 to delay the start of the biodegradation phase (time from the lag period to the 90% of maximum
334 biodegradation). A plateau was reached in all samples, after around 30 days, which represents the
335 maximum degradation values reached for each sample. The initial lag period for MCC sample was
336 similar to those found by others authors [28]. For the multilayers, this period was longer than those
337 found in the literature for cast starch based films [28]. This could be due to the different film thickness
338 and polymer structure or crystalline content, affected by the film's processing method. SPS displayed
339 a shorter initial lag period than SS films, probably because of the lack of adherence among hydrophilic
340 (SS) and hydrophobic (PCL) layers [37] in the moist environment, where starch layers swelled
341 promoting the multilayer detachment throughout the process. This enhances the specific film surface
342 area and biodegradation rate. The effect of specific surface area on the biodegradation behaviour of
343 films has also been previously reported by other authors [38].



345 **Figure 4.** Biodegradation kinetics of MCC and the different films with and without carvacrol throughout
346 the composting time. Experimental data (symbols) and Hill's fitted model (lines).

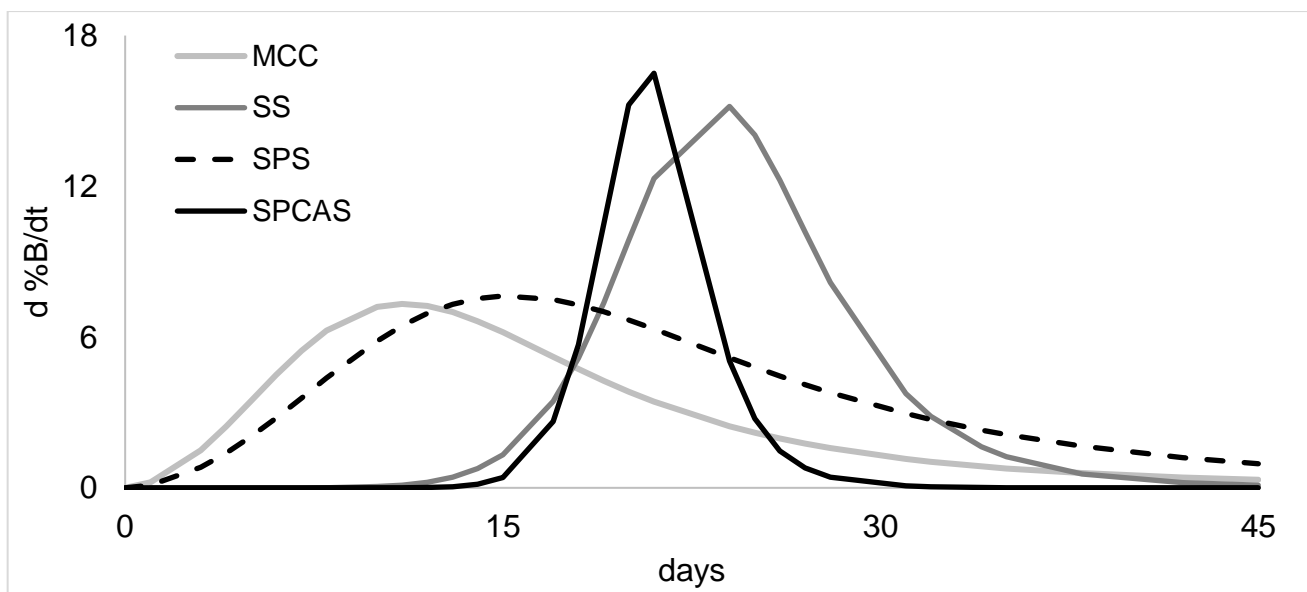
347

348 For starch and cellulose, amylases and cellulases are responsible for the cleavage of glycosidic bonds
349 [39]. The degradation of PCL mainly takes place by enzymatic hydrolytic ester cleavage, which is
350 attributed to microorganisms that secrete extracellular PCL depolymerases such as esterase,
351 cutinase and lipase [40], [41], [42]. The PCL also undergoes hydrolytic degradation due to the
352 presence of hydrolytically labile aliphatic ester linkages, but this degradation is rather slow because
353 of the hydrophobic nature of PCL [43]. After 25 days, biodegradation of the reference sample (MCC)
354 was greater than 70%, thus meeting the requirements established by the ISO 14855 standard [31],
355 and the CA-free film samples reached values of around 100 % of biodegradation ($B_{25}\%$ values, **Table**
356 **4**). The biodegradation experimental values were fitted by the Hill's model, and the obtained
357 parameters are shown in **Table 4**. As can be observed, MCC, SS and SPS films reached maximum
358 biodegradation values greater than 100% (curve plateau), which can be due to the priming effect. This
359 effect occurs when the compost inoculum in the samples' reactors produces more CO_2 than the one
360 in the blank reactors [44], as microflora is overstimulated by small molecules being released into the
361 medium as consequence of the polymer degradation. This effect was not observed in samples
362 containing carvacrol. In fact, SPCAS was not fully degraded during the composting period, reaching
363 a B_{max} (%) value of around 85 %, which can be attributed to the antimicrobial effect of carvacrol. This
364 effect could limit the growth of the microbial community and its biodegradation action on the films
365 (longer lag period and lower maximum degradation). In fact, the CA loaded electrospun PCL fibres in
366 multilayer films have been reported to exert an effective antimicrobial action due to the CA diffusion
367 into the starch layers [14]. So, the partial migration of the carvacrol to the starch layers in the
368 multilayer assembly will affect biodegradation of both PCL and S sheets, thus reaching lower final
369 biodegradation values. Other studies carried out with starch and gluten films incorporating active
370 essential oils showed that the presence of these antimicrobials did not significantly inhibit the
371 biodegradation process of the films [27], [28]. In these cases, the use of hydrophilic films, which
372 absorb water easily, contributed to the plasticization of the polymer matrix and thus, to the fast
373 antimicrobial compound release and volatilization, and so, it doesn't affect the microbial assimilation
374 of the films under composting exposure. In contrast, the presence of carvacrol in the multilayer
375 assembly with greater thickness seems to increase the persistence of the antimicrobial in the films,
376 thus partially inhibiting the microbial action and the enzyme access to the polymer, further limiting the
377 biodegradation processes.

378 **Table 4.** Hill's parameters: n , k (the time needed for 50 % of B_{max} to occur), B_{max} (percentage of
379 biodegradation at infinite time), B_{25} (percentage of biodegradation after 25 days) maximum
380 biodegradation rate (τ_{max}), time at this maximum ($t_{\tau_{max}}$) for the different films and microcrystalline
381 cellulose (MCC, reference) and R^2 (correlation coefficient for the fitted model).

| Sample | n | k (days) | B _{max} (%) | B ₂₅ (%) | τ _{max} (%B/day) | t _{τ max} (days) | R ² |
|--------|------|----------|----------------------|---------------------|---------------------------|---------------------------|----------------|
| MCC | 2.8 | 14.5 | 134 | 110 | 7.3 | 11 | 0.90 |
| SS | 9.1 | 24.0 | 160 | 95 | 15.2 | 24 | 0.85 |
| SPS | 2.8 | 19.8 | 188 | 124 | 7.6 | 15 | 0.96 |
| SPCAS | 16.2 | 20.9 | 85 | 81 | 16.5 | 21 | 0.80 |

382 **Figure 5** shows the biodegradation rates obtained from the first derivative of Hill's equation as a
383 function of time for each sample. In **Table 4**, the maximum biodegradation rate (τ_{max}) and the time
384 needed to reach this maximum ($t_{\tau max}$) value are shown. SS bilayer exhibited greater degradation
385 rates than SPS (around 15.2 and 7.6 %B/day, respectively) but delayed in time. This can be attributed
386 to the greatest adhesion force between the two starch layers in the SS assembly that limit the water
387 diffusion between layers, making the greater sample thickness more effective than in the SPS
388 assembly. In the latter, the starch swelling in the wet ambient should enhance the detachment of the
389 layers, reducing the effective thickness of the multilayer. This should favour a more extended
390 biodegradation process with lower maximum biodegradation rate, in line with the progressive increase
391 in the specific surface area of the multilayer assembly. Additionally, the polyester enzymatic
392 degradation (leading to small organic acid fractions) could also affect the biochemical route of starch
393 degradation. SPS films with and without carvacrol exhibited different maximum biodegradation rates
394 (16.5 and 7.6 %B/day, respectively) and these values were reached at different incubation times (21
395 and 15 days for SPCAS and SPS, respectively). So, those films incorporating CA needed a longer
396 composting exposure time to reach the maximum biodegradation rate than those films without the
397 antimicrobial agent. This could be attributed to the time necessary for carvacrol volatilization and the
398 subsequent reduction of its inhibitory effect.



400 **Figure 5.** Biodegradation rates of MCC and the different films with and without carvacrol throughout
401 the composting time.

402

403 **4. Conclusion**

404 All multilayer films (containing or not CA) exhibited the same trend of disintegration throughout the
405 composting exposure time. The biodegradation process of pure bilayer starch films was retarded, in
406 comparison with starch-PCL multilayer, by the greater effective thickness of the bilayer, due to the
407 highest adhesion forces between the starch sheets. In contrast, starch-PCL multilayers, exhibited an
408 earlier, more extended degradation behaviour with lower peak rate. The biodegradation test revealed
409 that the presence of CA notably affected the compost inoculum activity, thus limiting the
410 biodegradability of the CA-loaded multilayers to a maximum value of around 85 %. Nevertheless, the
411 biodegradation values reached by the CA loaded films were very close to that established by the
412 standard ISO method to be considered as biodegradable material (90 %). Further biodegradation
413 studies under longer composting times are recommended to evaluate the total biodegradation of
414 carvacrol-loaded SPS films.

415

416 **5. Acknowledgements**

417 The authors thank the Ministerio de Economía y Competitividad (MINECO, Spain) for funding this
418 study through the pre-doctoral grant BES-20014-068100 and through the investigation project
419 AGL2016-76699-R.

420

421 **6. References**

422 [1]. R. C. Thompson, C. J. Moore, F. S. vom Saal, S. H. Swan. Plastics, the environment and human
423 health: current consensus and future trends 364. *Phil. Trans. R. Soc. B* 364 (2009) 1526.
424 <http://doi.org/10.1098/rstb.2009.0053>

425 [2]. www.epa.gov (page accessed in May 2019)

426 [3]. <http://www.e-pro-plasticsrecycling.org> (page accessed in May 2019).

427 [4]. S. Jahan, V. Strezov, H. Weldekidan, R. Kumar, T. Kan, S.A. Sarkodie, J. He, B. Dastjerdi, S.P.
428 Wilson, Interrelationship of microplastic pollution in sediments and oysters in a seaport environment
429 of the eastern coast of Australia, *Sci. Total Environ.* 695 (2019) 133924.
430 [doi:10.1016/j.scitotenv.2019.133924](https://doi.org/10.1016/j.scitotenv.2019.133924).

431 [5]. J. Li, X. Qu, L. Su, W. Zhang, D. Yang, P. Kolandhasamy, D. Li, H. Shi, Microplastics in mussels
432 along the coastal waters of China, *Environ. Pollut.* 214 (2016) 177–184.
433 [doi:10.1016/j.envpol.2016.04.012](https://doi.org/10.1016/j.envpol.2016.04.012).

434 [6]. M. Renzi, C. Guerranti, A. Blašković, Microplastic contents from maricultured and natural mussels,
435 *Mar. Pollut. Bull.* 131 (2018) 248–251. [doi:10.1016/j.marpolbul.2018.04.035](https://doi.org/10.1016/j.marpolbul.2018.04.035).

436 [7]. M.F.M. Santana, L.G. Ascer, M.R. Custódio, F.T. Moreira, A. Turra, Microplastic contamination in
437 natural mussel beds from a Brazilian urbanized coastal region: Rapid evaluation through
438 bioassessment, *Mar. Pollut. Bull.* 106 (2016) 183–189. doi:10.1016/j.marpolbul.2016.02.074.

439 [8]. A.J.R. Watts, M.A. Urbina, S. Corr, C. Lewis, T.S. Galloway, Ingestion of Plastic Microfibers by
440 the Crab *Carcinus maenas* and Its Effect on Food Consumption and Energy Balance, *Environ. Sci.*
441 *Technol.* 49 (2015) 14597–14604. doi:10.1021/acs.est.5b04026.

442 [9]. Jinhui, X. Sudong, N. Yan, P. Xia, Q. Jiahao, X. Yongjian, Effects of microplastics and attached
443 heavy metals on growth, immunity, and heavy metal accumulation in the yellow seahorse,
444 *Hippocampus kuda Bleeker*, *Mar. Pollut. Bull.* 149 (2019) 110510.
445 doi:10.1016/j.marpolbul.2019.110510.

446 [10]. R. Qiao, Y. Deng, S. Zhang, M.B. Wolosker, Q. Zhu, H. Ren, Y. Zhang, Accumulation of different
447 shapes of microplastics initiates intestinal injury and gut microbiota dysbiosis in the gut of zebrafish,
448 *Chemosphere.* 236 (2019) 124334. doi:10.1016/j.chemosphere.2019.07.065.

449 [11]. EFSA CONTAM Panel (EFSA Panel on Contaminants in the Food Chain) Statement on the
450 presence of microplastics and nanoplastics in food, with particular focus on seafood EFSA J., 14 (6)
451 (2016), pp. 4501-4531

452 [12]. A. Heimowska, M. Morawska, A. Bocho-Janiszewska, Biodegradation of poly(ϵ -caprolactone) in
453 natural water environments, *Polish J. Chem. Technol.* 19 (2017) 120–126. doi:10.1515/pjct-2017-
454 0017.

455 [13]. R. Ortega-Toro, J. Contreras, P. Talens, A. Chiralt., Physical and structural properties and
456 thermal behaviour of starch-poly(ϵ -caprolactone) blend films for food packaging, *Food Packag. Shelf*
457 *Life.* 5 (2015) 10–20. doi:10.1016/j.fpsl.2015.04.001.

458 [14]. A. Tampau, C. González-Martínez, A. Chiralt, Release kinetics and antimicrobial properties of
459 carvacrol encapsulated in electrospun poly-(ϵ -caprolactone) nanofibres. Application in starch
460 multilayer films, *Food Hydrocoll.* 79 (2018) 158–169. doi:10.1016/j.foodhyd.2017.12.021.

461 [15]. A. Tampau, C. González-Martínez, A. Chiralt, Carvacrol encapsulation in starch or PCL based
462 matrices by electrospinning, *J. Food Eng.* 214 (2017) 245–256. doi:10.1016/j.jfoodeng.2017.07.005.

463 [16]. M. Ramos, A. Jiménez, M. Peltzer, M.C. Garrigós, Characterization and antimicrobial activity
464 studies of polypropylene films with carvacrol and thymol for active packaging, *J. Food Eng.* 109 (2012)
465 513–519. doi:10.1016/j.jfoodeng.2011.10.031.

466 [17]. A. Ben Arfa, L. Preziosi-Belloy, P. Chalier, N. Gontard, Antimicrobial paper based on a soy
467 protein isolate or modified starch coating including carvacrol and cinnamaldehyde, *J. Agric. Food*
468 *Chem.* 55 (2007) 2155–2162. doi:10.1021/jf0626009.

469 [18]. A. Ultee, M.H.J. Bennik, R. Moezelaar, The phenolic hydroxyl group of carvacrol is essential for
470 action against the food-borne pathogen *Bacillus cereus*, *Appl. Environ. Microbiol.* 68 (2002) 1561–
471 1568. doi:10.1128/AEM.68.4.1561-1568.2002.

472 [19]. S. Tunc, E. Chollet, P. Chalier, L. Preziosi-Belloy, N. Gontard, Combined effect of volatile
473 antimicrobial agents on the growth of *Penicillium notatum*, *Int. J. Food Microbiol.* 113 (2007) 263–270.
474 doi:10.1016/j.ijfoodmicro.2006.07.004.

475 [20]. B. Tepe, M. Sokmen, H.A. Akpulat, D. Daferera, M. Polissiou, A. Sokmen, Antioxidative activity
476 of the essential oils of *Thymus sipyleus subsp. sipyleus var. sipyleus* and *Thymus sipyleus subsp.*
477 *sipyleus var. rosulans*, *J. Food Eng.* 66 (2005) 447–454. doi:10.1016/j.jfoodeng.2004.04.015.

478 [21]. S. Gursul, I. Karabulut, G. Durmaz, Antioxidant efficacy of thymol and carvacrol in
479 microencapsulated walnut oil triacylglycerols, *Food Chem.* 278 (2019) 805–810.
480 doi:10.1016/j.foodchem.2018.11.134.

481 [22]. Joint FAO/WHO Expert Committee on Food Additives Fifty-seventh meeting Rome, 5-14 June
482 2001, (2001).

483 [23]. Efsa, Scientific Opinion on the Safety and efficacy of phenol derivates containing ring-alkyl, ring-
484 alkoxy and side- chains with an oxygenated functional group (chemical group 25) when used as
485 flavourings for all species, *Efsa J.* 10 (2012) 2573. doi:10.2903/j.efsa.2012.2573.

486 [24]. G. Kavooosi, S.M.M. Dadfar, A. Mohammadi Purfard, R. Mehrabi, Antioxidant and antibacterial
487 properties of gelatin films incorporated with carvacrol, *J. Food Saf.* 33 (2013) 423–432.
488 doi:10.1111/jfs.12071.

489 [25]. M.A. López-Mata, S. Ruiz-Cruz, N.P. Silva-Beltrán, J.D.J. Ornelas-Paz, P.B. Zamudio-Flores,
490 S.E. Burruel-Ibarra, Physicochemical, antimicrobial and antioxidant properties of chitosan films
491 incorporated with carvacrol, *Molecules.* 18 (2013) 13735–13753. doi:10.3390/molecules181113735.

492 [26]. L. Higuera, G. López-Carballo, P. Hernández-Muñoz, R. Catalá, R. Gavara, Antimicrobial
493 packaging of chicken fillets based on the release of carvacrol from chitosan/cyclodextrin films, *Int. J.*
494 *Food Microbiol.* 188 (2014) 53–59. doi:10.1016/j.ijfoodmicro.2014.07.018.

495 [27]. M.P. Balaguer, J. Villanova, G. Cesar, R. Gavara, P. Hernandez-Munoz, Compostable properties
496 of antimicrobial bioplastics based on cinnamaldehyde cross-linked gliadins, *Chem. Eng. J.* 262 (2013)
497 447–455. doi:10.1016/j.cej.2014.09.099.

498 [28]. A.I. Cano, M. Cháfer, A. Chiralt, C. González-Martínez, Biodegradation behavior of starch-PVA
499 films as affected by the incorporation of different antimicrobials, *Polym. Degrad. Stab.* 132 (2016) 11–
500 20. doi:10.1016/j.polymdegradstab.2016.04.014.

501 [29]. European Union, European Parliament and Council Directive 94/62/EC on Packaging and
502 Packaging Waste, *Off. J. Eur. Communities No L 365/10.* 1993 (1994) 10–23.
503 doi:10.1038/sj.bdj.4811054.

504 [30]. ISO 20200, *Plastics - Determination of the Degree of Disintegration of Plastic Materials under*
505 *Simulated Composting in a Laboratory-scale Test*, 2004.

506 [31]. UNE-EN ISO 14855-1, *Determinación de la biodegradabilidad aeróbica final de materiales*
507 *plásticos en condiciones de compostaje controladas*, in: *Método según el análisis de dióxido de*
508 *carbono generado*, 2012. Parte 1: Método general.

509 [32]. E. Talón, M. Vargas, A. Chiralt, C. González-Martínez, Eugenol incorporation into
510 thermoprocessed starch films using different encapsulating materials, *Food Packag. Shelf Life*. 21
511 (2019) 100326. doi:10.1016/j.fpsl.2019.100326.

512 [33]. E. Castro-Aguirre, R. Auras, S. Selke, M. Rubino, T. Marsh, Insights on the aerobic
513 biodegradation of polymers by analysis of evolved carbon dioxide in simulated composting conditions,
514 *Polym. Degrad. Stab.* 137 (2017) 251–271. doi:10.1016/j.polymdegradstab.2017.01.017.

515 [34]. S. Collazo-Bigliardi, R. Ortega-Toro, A. Chiralt, Reinforcement of thermoplastic starch films with
516 cellulose fibres obtained from rice and coffee husks, *J. Renew. Mater.* 6 (2018) 599–610.
517 doi:10.32604/JRM.2018.00127.

518 [35]. P.A. Sreekumar, M.A. Al-Harhi, S.K. De, Studies on compatibility of biodegradable
519 starch/polyvinyl alcohol blends, *Polym. Eng. Sci.* 52 (2012) 2167–2172. doi:10.1002/pen.23178.

520 [36]. E. Rudnik, Biodegradability testing of compostable polymer materials, in: *Compost. Polym.*
521 *Mater*, Elsevier, 2008: pp. 112–166. doi:10.1016/B978-008045371-2.50008-1.

522 [37]. R.P. Singh, J.K. Pandey, D. Rutot, P. Degée, P. Dubois, Biodegradation of poly(ϵ -
523 caprolactone)/starch blends and composites in composting and culture environments: The effect of
524 compatibilization on the inherent biodegradability of the host polymer, *Carbohydr. Res.* 338 (2003)
525 1759–1769. doi:10.1016/S0008-6215(03)00236-2.

526 [38]. H.S. Yang, J.S. Yoon, M.N. Kim, Dependence of biodegradability of plastics in compost on the
527 shape of specimens, *Polym. Degrad. Stab.* 87 (2005) 131–135.
528 doi:10.1016/j.polymdegradstab.2004.07.016.

529 [39]. B.P. Wasserman, *Principles of enzymology for the food sciences*, 2nd edition. John R. Whitaker,
530 Marcel Dekker, Inc., 270 Madison Ave., New York, NY 10016. 1994. 648 pages. \$185.00, *J. Food*
531 *Saf.* 15 (1995) 365a – 366. doi:10.1111/j.1745-4565.1995.tb00147.x.

532 [40] C.A. Murphy, J.A. Cameron, S.J. Huang, R.T. Vinopal, *Fusarium* polycaprolactone depolymerase
533 is cutinase, *Appl. Environ. Microbiol.* 62 (1996) 456–460.

534 [41] C.A. Murphy, J.A. Cameron, S.J. Huang, R.T. Vinopal, A second polycaprolactone depolymerase
535 from *Fusarium*, a lipase distinct from cutinase, *Appl. Microbiol. Biotechnol.* 50 (1998) 692–696.
536 doi:10.1007/s002530051352.

537 [42] Y. Tokiwa, B.P. Calabia, C.U. Ugwu, S. Aiba, Biodegradability of plastics, *Int. J. Mol. Sci.* 10
538 (2009) 3722–3742. doi:10.3390/ijms10093722.

539 [43] A. Banerjee, K. Chatterjee, G. Madras, Enzymatic degradation of polycaprolactone-gelatin blend,
540 *Mater. Res. Express.* 2 (2015). doi:10.1088/2053-1591/2/4/045303.

541 [44] J. Shen, R. Bartha, Priming effect of glucose polymers in soil-based biodegradation tests, *Soil*
542 *Biol. Biochem.* 29 (1997) 1195–1198. doi:10.1016/S0038-0717(97)00031-X.